J|A|C|S
ARTICLES

Published on Web 11/02/2009

Large Magnetization-Induced Second Harmonic Generation in an Enantiopure Chiral Magnet

Cyrille Train,*[,†,‡,§] Tomohiro Nuida,[†] Ruxandra Gheorghe,[‡] Michel Gruselle,[‡] and Shin-ichi Ohkoshi*[,†]

Department of Chemistry, School of Science, The University of Tokyo, 7-3-1 Hongo, Bunkyo-ku, Tokyo 113-0033, Japan, Institut Parisien de Chimie Moléculaire, UMR CNRS 7201, UPMC Univ Paris 06, case 42, 4 place Jussieu, F-75252 Paris Cedex 05, France, and Laboratoire National des Champs Magnétiques Intenses, UPR CNRS 3228, 25 rue des Martyrs, B.P. 166, 38042 Grenoble Cedex 9, France

Received July 23, 2009; E-mail: cyrille.train@grenoble.cnrs.fr; ohkoshi@chem.s.u-tokyo.ac.jp

Abstract: The absence of centrosymmetry in the enantiopure chiral magnet $[N(CH_3)(n\text{-}C_3H_7)_2(C^*H(CH_3)C_2H_5)][Mn^{II}Cr^{III}(ox)_3]$ allows the observation of *bulk* second harmonic generation (SHG) in this material. At low temperature, the onset of magnetization gives birth to a magnetization-induced SHG (MSHG) contribution. With an angular shift of 13.1° upon magnetization reversal, the MSHG effects appear to be much larger than the corresponding linear magneto-optical effects. Thanks to the single-crystalline state of the sample, the variation of the signal with the orientation of the magnetic field and/or the angle between the polarization of the incident radiation and the outgoing SHG signal in the paramagnetic and ferromagnetic phases is reproduced and well-understood through the use of a symmetry-based analysis of the nonlinear susceptibility tensor.

Introduction

One of the current trends in molecular magnetism and throughout materials science is to synthesize and study multifunctional magnetic compounds.[1] The association[2,3] or interaction[4−6] between two physicochemical properties is of fundamental interest in discovering and/or experimenting with new physicochemical properties and in particular could give rise to original solutions in data-storage applications.

In addition to the magnetic ordering, which is related to the breaking of time-reversal symmetry,[7] considerable effort has been devoted to introducing properties related to the loss of parity-reversal symmetry. The importance of breaking the latter symmetry in magnetic materials is obvious when magnetochiral dichroism (MChD) is considered,[6,8] but as a direct consequence of tensor symmetry analysis, it is also requisite for the appearance of ferroelectricity, second harmonic generation (SHG), and related properties.[7]

Two strategies can be followed to obtain (magnetic) noncentrosymmetric materials. The first one, which is not restricted to molecular chemistry, relies on a careful analysis of (published) X-ray data to track the occurrence of noncentrosymmetric space groups eventually upon a decrease in temperature. This strategy allows one to identify the possible candidates and, through chemical substitution, obtain efficient materials for nonlinear optics (NLO),[9] ferroelectricity,[10] or multiferroicity.[11] In molecular magnetism, the exploitation of symmetry analysis in Prussian Blue analogues (PBAs) has led to the identification of compounds adapted for observing magnetization-induced SHG (MSHG) as well as materials combining magnetism with ferroelectricity or pyroelectricity.[3,4,12−15] As far as molecular

[†] The University of Tokyo.
[‡] Institut Parisien de Chimie Moléculaire, UMR CNRS 7201.
[§] Laboratoire National des Champs Magnétiques Intenses, UPR CNRS 3228.

(1) Verdaguer, M.; Gatteschi, D. *C. R. Chim.* **2008**, *11*, 1083.
(2) (a) Kurmoo, M.; Graham, A. W.; Day, P.; Coles, S. J.; Hursthouse, M. B.; Caulfield, J. L.; Singleton, J.; Pratt, F. L.; Hayes, W.; Ducasse, L.; Guionneau, P. *J. Am. Chem. Soc.* **1995**, *117*, 12209. (b) Coronado, E.; Galan-Mascaros, J. R.; Gomez-Garcia, C. J.; Laukhin, V. *Nature* **2000**, *408*, 447. (c) Andres, R.; Brissard, M.; Gruselle, M.; Train, C.; Vaissermann, J.; Malezieux, B.; Jamet, J.-P.; Verdaguer, M. *Inorg. Chem.* **2001**, *40*, 4633.
(3) Ohkoshi, S.; Tokoro, H.; Matsuda, T.; Takahashi, H.; Irie, H.; Hashimoto, K. *Angew. Chem., Int. Ed.* **2007**, *46*, 3238.
(4) Ikeda, K.; Ohkoshi, S.; Hashimoto, K. *Chem. Phys. Lett.* **2001**, *349*, 371.
(5) Eerenstein, W.; Mathur, N. D.; Scott, J. F. *Nature* **2006**, *442*, 759.
(6) Train, C.; Gheorghe, R.; Krstic, V.; Chamoreau, L.-M.; Ovanesyan, N. S.; Rikken, G. L. J. A.; Gruselle, M.; Verdaguer, M. *Nat. Mater.* **2008**, *7*, 729.
(7) Birss, R. R. *Symmetry and Magnetism*; North Holland: Amsterdam, 1964; Vol. 3.
(8) (a) Rikken, G. L. J. A.; Raupach, E. *Nature* **1997**, *390*, 493. (b) Rikken, G. L. J. A.; Raupach, E. *Phys. Rev. E* **1998**, *58*, 5081.
(9) (a) Benard, S.; Yu, P.; Audiere, J. P.; Riviere, E.; Clement, R.; Guilhem, J.; Tchertanov, L.; Nakatani, K. *J. Am. Chem. Soc.* **2000**, *122*, 9444. (b) Clement, R.; Decurtins, S.; Gruselle, M.; Train, C. *Monatsh. Chem.* **2003**, *134*, 117.
(10) (a) Scott, J. F. *Science* **2007**, *315*, 954. (b) Spaldin, N. A. In *Physics of Ferroelectrics: A Modern Perspective*; Springer: New York, 2007; p 175. (c) Horiuchi, S.; Tokura, Y. *Nat. Mater.* **2008**, *7*, 357.
(11) (a) Cheong, S. W.; Mostovoy, M. *Nat. Mater.* **2007**, *6*, 13. (b) Gajek, M.; Bibes, M.; Fusil, S.; Bouzehouane, K.; Fontcuberta, J.; Barthelemy, A. E.; Fert, A. *Nat. Mater.* **2007**, *6*, 296.
(12) (a) Ikeda, K.; Ohkoshi, S.; Hashimoto, K. *J. Electrochem. Soc.* **2002**, *149*, E445. (b) Hozumi, T.; Nuida, T.; Hashimoto, K.; Ohkoshi, S. *Cryst. Growth Des.* **2006**, *6*, 1736. (c) Kosaka, W.; Nuida, T.; Hashimoto, K.; Ohkoshi, S. *Bull. Chem. Soc. Jpn.* **2007**, *80*, 960.
(13) Ikeda, K.; Ohkoshi, S.; Hashimoto, K. *Electrochemistry* **2003**, *71*, 184.
(14) Ikeda, K.; Ohkoshi, S.; Hashimoto, K. *J. Appl. Phys.* **2003**, *93*, 1371.

 10.1021/ja9061568 CCC: $40.75

chemistry is concerned, a second strategy is possible. It relies on versatility in the choice of the building blocks to control the molecular arrangement as well as the spins in the material. In particular, using enantiomerically pure building blocks rules out the presence, in the solid state, of any improper symmetry element among the symmetry operations. Using enantioselective supramolecular self-assembly involving coordination bonds and/or weaker intermolecular interactions is thus a very efficient strategy for synthesizing noncentrosymmetric compounds.[16] Through association with spin bearers such as organic radicals or transition-metal or lanthanide ions, it has been possible to introduce magnetic properties and long-range magnetic ordering in enantiomerically pure compounds.[6,17] This strategy has recently been used to crystallize enantiomerically pure single crystals of a two-dimensional oxalate-based ferromagnet having the general formula $[N(CH_3)(n\text{-}C_3H_7)_2(C^*H(CH_3)C_2H_5)][Mn^{II}Cr^{III}(\mu\text{-}C_2O_4)_3]$ (designated as N*[MnCr]), which demonstrates the long-sought enhancement of MChD in the magnetically ordered state of an enantiomerically pure molecular material.[6]

Along these lines, we measured the SHG signal resulting from the noncentrosymmetry induced in N*[MnCr] by the enantioselective self-assembly process. The magnetization-induced variation of the signal was exemplified and precisely analyzed by a careful tensor analysis made possible by the single-crystalline state of the sample.

Experimental Section

Synthesis. The synthesis and crystallization conditions previously described[6,18] were used to obtain the single crystals of the studied compound.

Physical Measurements. The magnetic properties were measured on a Quantum Design MPMS5 SQUID magnetometer. The magnetic susceptibility of oriented single crystals was measured between 2 and 300 K in a 1.0 mT field. During the measurement of magnetization curves below the Curie temperature under the application of an external magnetic field parallel to the crystalline *c* axis, the magnet was reset every time the field crossed zero. The angular dependence of the magnetization of one single crystal at zero applied magnetic field was measured at 2 K after slow cooling at 1.0 mT.

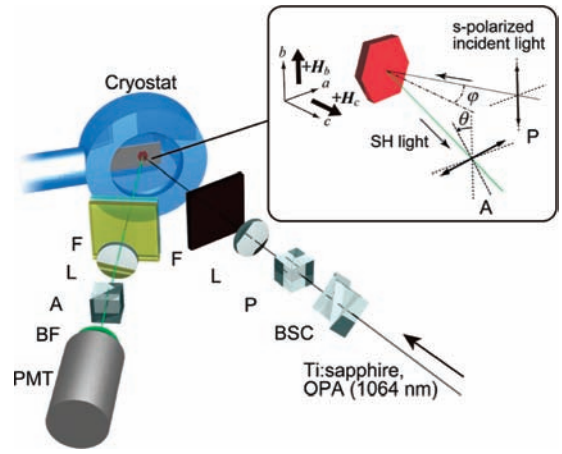

Figure 1. Experimental setup for (M)SHG measurements (BSC, Babinet−Soleil compensator; P, polarizer; L, lens; F, optical filter; S, sample; A, analyzer; BF, bandpass filter; PMT, photomultiplier tube).

The experimental setup used for the MSHG measurements is depicted in Figure 1. An optical parametric amplifier (Clark-MXR Vis-OPA; pulse width, 190 fs; repetition, 1 kHz) pumped by a frequency-doubled Ti:sapphire laser (Clark-MXR CPA-2001; wavelength, 775 nm; pulse width, 150 fs; repetition, 1 kHz) provided the incident radiation (1064 nm). The reflected SHG light (532 nm) was detected by a photomultiplier tube (Hamamatsu R329-02) through color filters. For temperature-dependent measurements, a cryostat (Oxford Microstat He) was used to control the temperature of the samples. A hexagonal-shaped N*[MnCr] single crystal was mounted in the cryostat, as shown in the inset of Figure 1. An aluminum sample holder was used in order to ensure efficient thermalization of the sample. The angle of incidence and reflection on the sample (φ) was fixed at 20°. Thanks to the Babinet−Soleil compensator (BSC) and polarizer (P), the polarization of the incident light was kept along the *Y* axis (s-polarized). The analyzer (A) could be introduced into the experimental setup in order to perform the polarization analysis of the SHG output signal. The angle between the polarizer and the analyzer is denoted as θ. The magnetic field was applied along the *b* or *c* direction using permanent magnets.

Results

In a first series of experiments, the magnetization variations under the application of an external magnetic field were measured below the Curie temperature (T_C) of the compound. Since the compound is known to be a very soft magnet,[6] the coercive force was determined with utmost attention in order to extract reliable values. It thus appears that the coercive force is as low as 0.3 mT at 2 K and drops to zero at 6 K (Figure 2a). The results of this accurate study quantitatively show that the magnetocrystalline anisotropy of the compound is very low. This is understandable given the weakness of the single-ion anisotropy of sixfold-coordinate manganese(II) and chromium(III) ions. Moreover, the low values of the coercive force indicate that application of low external fields can be used to modify the orientation of the magnetization in the sample.

A second piece of information that is essential for precise tensorial analysis of the MSHG is the orientation of the magnetization at zero field. To determine the easy axis of N*[MnCr], the rotational dependence of the magnetization at

(15) Nuida, T.; Matsuda, T.; Tokoro, H.; Sakurai, S.; Hashimoto, K.; Ohkoshi, S. *J. Am. Chem. Soc.* **2005**, *127*, 11604.
(16) (a) Kawamata, J.; Ogata, Y.; Taniguchi, M.; Yamagishi, A.; Inoue, K. *Mol. Cryst. Liq. Cryst.* **2000**, *343*, 371. (b) Jouaiti, A.; Hosseini, M. W.; Kyritsakas, N. *Chem. Commun.* **2002**, 1898. (c) Ok, K. M.; Chi, E. O.; Halasyamani, P. S. *Chem. Soc. Rev.* **2006**, *35*, 710. (d) Ye, Q.; Fu, D.-W.; Tian, H.; Xiong, R.-G.; Chan, P. W. H.; Huang, S. D. *Inorg. Chem.* **2008**, *47*, 772. (e) Crassous, J. *Chem. Soc. Rev.* **2009**, *38*, 830.
(17) (a) Inoue, K.; Imai, H.; Ghalsasi, P. S.; Kikuchi, K.; Ohba, M.; Okawa, H.; Yakhmi, J. V. *Angew. Chem., Int. Ed.* **2001**, *40*, 4242. (b) Inoue, K.; Kikuchi, K.; Ohba, M.; Okawa, H. *Angew. Chem., Int. Ed.* **2003**, *42*, 4810. (c) Imai, H.; Inoue, K.; Kikuchi, K.; Yoshida, Y.; Ito, M.; Sunahara, T.; Onaka, S. *Angew. Chem., Int. Ed.* **2004**, *43*, 5618. (d) Zhang, B.; Wang, Z. M.; Kurmoo, M.; Gao, S.; Inoue, K.; Kobayashi, H. *Adv. Funct. Mater.* **2007**, *17*, 577. (e) Minguet, M.; Luneau, D.; Lhotel, E.; Villar, V.; Paulsen, C.; Amabilino, D. B.; Veciana, J. *Angew. Chem., Int. Ed.* **2002**, *41*, 586. (f) Clemente-Leon, M.; Coronado, E.; Gomez-Garcia, C. J.; Soriano-Portillo, A. *Inorg. Chem.* **2006**, *45*, 5653. (g) Coronado, E.; Gomez-Garcia, C. J.; Nuez, A.; Romero, F. M.; Waerenborgh, J. C. *Chem. Mater.* **2006**, *18*, 2670. (h) Clemente-Leon, M.; Coronado, E.; Dias, J. C.; Soriano-Portillo, A.; Willett, R. D. *Inorg. Chem.* **2008**, *47*, 6458. (i) Pointillart, F.; Train, C.; Gruselle, M.; Villain, F.; Schmalle, H. W.; Talbot, D.; Gredin, P.; Decurtins, S.; Verdaguer, M. *Chem. Mater.* **2004**, *16*, 832. (j) Gruselle, M.; Thouvenot, R.; Malezieux, B.; Train, C.; Gredin, P.; Demeschik, T. V.; Troitskaya, L. L.; Sokolov, V. I. *Chem.—Eur. J.* **2004**, *10*, 4763. (k) Pointillart, F.; Train, C.; Boubekeur, K.; Gruselle, M.; Verdaguer, M. *Tetrahedron: Asymmetry* **2006**, *17*, 1937. (l) Pointillart, F.; Train, C.; Villain, F.; Cartier dit Moulin, C.; Gredin, P.; Chamoreau, L. M.; Gruselle, M.; Aullon, G.; Alvarez, S.; Verdaguer, M. *J. Am. Chem. Soc.* **2007**, *129*, 1327.
(18) Gheorghe, R.; Chamoreau, L. M.; Kapitan, J.; Ovanesyan, N. S.; Aldoshin, S. M.; Hecht, L.; Barron, L. D.; Train, C.; Gruselle, M. *Chirality* **2008**, *20*, 1085.

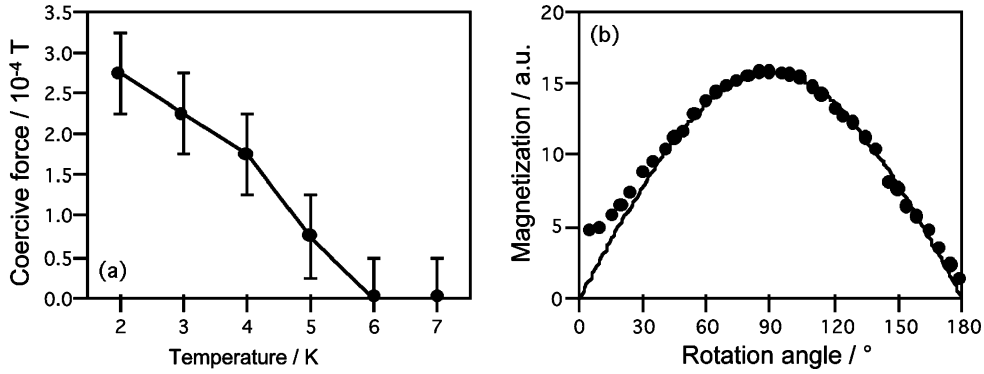

Figure 2. Magnetic properties of N*[MnCr]. (a) Thermal variations of the coercive force. (b) Angular dependence of the magnetization measured at zero field at 2 K (0° is parallel to the *ab* plane, and 90° is parallel to the *c* axis).

zero field was measured at 2 K (Figure 2b). It was found that the magnetization is maximized along the *c* axis, which is thus the easy axis of the material. These measurements compare well with previous experimental reports based on angle-dependent magnetometry or powder neutron diffraction on racemic[19] or enantiomerically pure[20] C[MCr] compounds [C = $N(C_3H_7)_4^+$, $P(C_6D_5)_4^+$]. The orientation of the easy axis perpendicular to the honeycomb bimetallic layers in [MCr] oxalate-based 2D networks thus appears to be independent of both the counterion and the enantiomeric purity. These accurate magnetic characterizations form a solid basis for a correct interpretation of the expected MSHG signal in N*[MnCr].

The SHG intensity of the powdered sample was measured at 293 K as the intensity of the incident light was increased (see the Supporting Information). The quadratic variation of the collected signal is the signature of its SHG origin. Comparison with the signal measured under the same conditions in potassium dihydrogen phosphate (KDP) led to a quantitative determination of the SHG susceptibility of 3.60×10^{-10} esu at 1064 nm.

The thermal variation of the SHG signal was measured for a single crystal of N*[MnCr] in a 30 mT magnetic field applied along the *c* axis (Figure 3a). Between 50 and 12 K, the SHG signal stayed constant within experimental error. It then increased by 40% as the temperature was further decreased to 2 K. The temperature dependence of the SHG signal follows the thermal evolution of the magnetization of the compound (Figure 3b).

Exploitation of the single-crystalline state of the sample allowed the magnetization to be reversed along the *b* axis (Figure 1) by applying a ±170 mT external magnetic field. Then the SHG intensity was measured as a function of the angle θ between the polarizer P and the analyzer A (Figure 1) above (20 K) and below (2 K) the Curie temperature of N*[MnCr] (Figure 4). Above T_C, within experimental error, the SHG intensity was independent of the external field orientation with respect to both its intensity and its angular variation (Figure 4a). The polarization analysis of the SHG intensity above T_C showed that the signal was maximized at $\theta = \pm 90°$ for crossed polarizations ($S_{in}-P_{out}$) and minimized at $\theta = 0°$ for parallel polarizations ($S_{in}-S_{out}$). Below T_C, the orientation of the external magnetic field acts on both the angular dependence and the intensity of the SHG signal (Figure 4b): the minimum signal was found at an extinction angle that changed from $\theta_{H_+} = -8.9°$ to $\theta_{H_-} = +4.2°$ when the field was reversed from +170 mT to −170 mT, and the maximum intensity in the negative applied magnetic field, I_{H_-}, was increased by >30% relative to the value in the positive applied magnetic field, I_{H_+}.

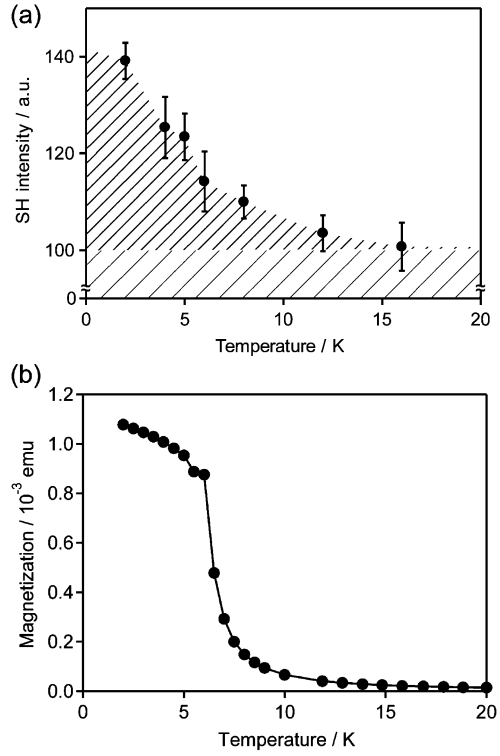

Figure 3. (a) Thermal variation of the SHG signal for a single crystal of N*[MnCr] in a 30 mT magnetic field applied along the *c*-axis. (b) Field-cooled curve in a 1.0 mT field applied along the *c* axis.

Discussion

The SHG susceptibility at 293 K for an emitted wavelength of 532 nm is 39% that of KDP. This value is much higher than the value observed in noncentrosymmetric PBAs.[12] It emphasizes the interest in using enantiomerically pure building blocks to synthesize noncentrosymmetric magnets. The enhancement of the SHG intensity when the material enters its ferromagnetic phase (Figure 3) is related to the modification of the second-order nonlinear susceptibility tensor upon the appearance of a nonzero magnetization.[15] The shift of the extinction angle upon field reversal (Figure 4b) is 5 times greater than that observed for $Fe_{0.5}Cr[Cr(CN)_6]\cdot 7.5H_2O$.[14]

(19) Pellaux, R.; Schmalle, H. W.; Huber, R.; Fischer, P.; Hauss, T.; Ouladdiaf, B.; Decurtins, S. *Inorg. Chem.* **1997**, *36*, 2301.
(20) Train, C.; Pointillart, F.; André, G. Unpublished results.

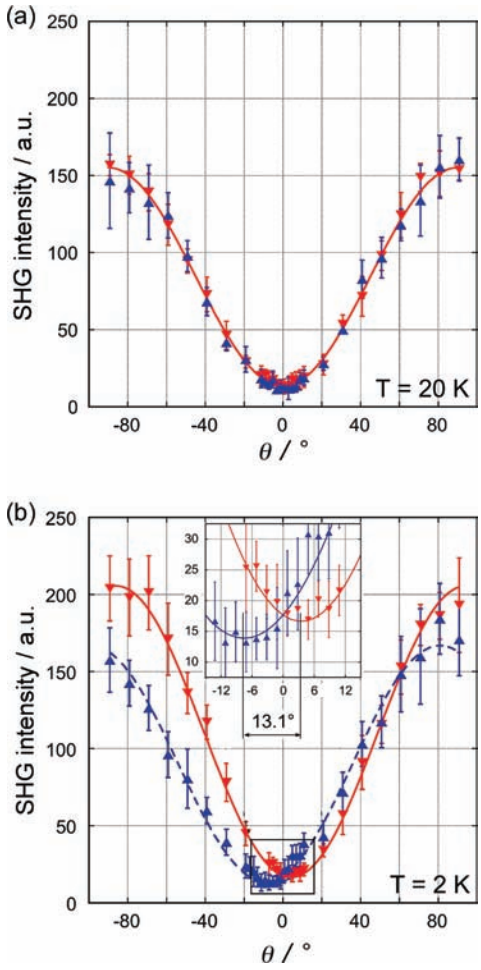

Figure 4. Polarization analysis of the SHG signals measured at (a) 20 and (b) 2 K with external fields of (▲) +170 and (▼) −170 mT applied along the *b* direction. The inset emphasizes the angular dependence of the minimum intensity upon orientation of the magnetization. The lines correspond to the fit of the experimental data to eq 1 (see the text).

The current study was essentially performed on a single crystal. Through the use of a simple model that assumes the (M)SHG effects to be solely related to hyperpolarizability, mastering the relative orientation of the crystallographic and optical frames allows the exploration of the possible contributions from the different terms of the hyperpolarizability tensor to the (M)SHG in an accurate way. Above T_C, the SHG intensity arises solely from the crystalline contribution. The crystallographic space group of N*[MnCr] is $P6_3$ which is related to the 6 point group. The nonzero terms of the third-rank nonlinear polarizability χ^{cr} in this point group are given in the Supporting Information. Incident light polarized along the *Y* direction of the optical frame, parallel to the *b* axis of the single crystal, is characterized by its electric field E_b. The nonzero contribution to the nonlinear polarization is then aligned along *c* and is equal to $\chi^{cr}_{cbb}E_b^2$. To calculate the SHG intensity, it is necessary to project the SHG polarization in the *XY* plane, perpendicular to the propagation direction of the SHG beam. In the present case, this projection is along the *X* direction and is equal to $\chi^{cr}_{cbb}E_b^2 \sin\varphi$ (Figure 5a). The SHG intensity I_{SHG} is then proportional to $|\chi^{cr}_{cbb}|^2 \sin^2\varphi$. When an analyzer is inserted into the experimental setup (Figure 1), the angular dependence of the SHG intensity is $|\chi^{cr}_{cbb}|^2 \sin^2\varphi \sin^2\theta$, which is minimized for $\theta = 0°$, as observed in Figure 4a.

Below T_C, a magnetic contribution adds to the crystalline one. This contribution is strongly dependent upon the orientation of the magnetization. The presence of spontaneous magnetization indeed causes the breaking of time-reversal symmetry and may result in the loss of some spatial symmetry operations as well, leading to less-symmetric space and point groups (see the Supporting Information).[7,21] In the first experiment (Figure 3), the field was applied along the *c* axis of the material. Since the easy axis of N*[MnCr] was demonstrated to be the *c* axis, when the field was applied along this direction, the magnetization remained along this axis. From the symmetry analysis in magnetically ordered materials,[7,21] the magnetic space group in the ferromagnetic phase with the magnetization aligned along the sixfold helical axis is still $P6_3$. With such an orientation of the magnetization, the shape of the nonlinear susceptibility tensor is not influenced by the magnetization (see the Supporting Information). Indeed, in this configuration, the appearance of nonzero magnetization is expected to merely modulate the χ_{cbb} term of the total second-order susceptibility tensor, so χ_{cbb} is then the sum of a crystal contribution (denoted χ^{cr}_{cbb}) and a magnetic one (denoted χ^{mag}_{cbb}). These contributions are complex quantities. They can be written as $|\chi^{cr}_{cbb}| \exp(-i\alpha)$ and $|\chi^{mag}_{cbb}| \exp[-i(\alpha + \delta^{mag}_{cbb})]$. In fully transparent compounds, δ^{mag}_{cbb} is equal to $\pi/2$,[22] and the total contribution to the SHG intensity is proportional to $|\chi^{cr}_{cbb}|^2 + |\chi^{mag}_{cbb}|^2$. The entry of the materials into the ferromagnetic phase thus induces an increase in the SHG intensity, as observed in Figure 3.

When the external magnetic field is applied along the *b* axis, the magnetization is aligned along that direction. In such a configuration, the symmetry of the ferromagnetic compound is significantly lowered: with a sixfold axis perpendicular to the *ab* plane, the *a* and *b* directions indeed play an equivalent role, but this is obviously not the case when the magnetization is oriented solely along the *b* axis (see the Supporting Information). As a result of the ferromagnetic nature of the long-range magnetic order, the magnetic space group becomes $P2_1$.[7,23] The χ^{mag}_{abb} and χ^{mag}_{bbb} terms can then be nonzero, while χ^{mag}_{cbb} is zero (see the Supporting Information). The determination of the SHG polarization is in this case more complicated and deserves to be described in detail. The projection of the SHG polarization in the *XY* plane (perpendicular to the propagation direction of the SHG wave) is $\chi^{mag}_{bbb}E_b^2$ in the *Y* direction and $(\chi^{mag}_{abb} \cos\varphi + \chi^{cr}_{cbb} \sin\varphi)E_b^2$ in the *X* direction (Figure 5b). The projection along the analyzer direction is thus $[\chi^{mag}_{bbb} \cos\theta + (\chi^{mag}_{abb} \cos\varphi + \chi^{cr}_{cbb} \sin\varphi) \sin\theta]E_b^2$. Taking into account the complex character of the terms of the nonlinear susceptibility tensor allows these quantities to be written as $|\chi^{cr}_{cbb}| \exp(i\alpha)$, $|\chi^{mag}_{abb}| \exp[-i(\alpha + \delta^{mag}_{abb})]$, and $|\chi^{mag}_{bbb}| \exp[-i(\alpha + \delta^{mag}_{bbb})]$, where $|\chi^{mag}_{abb}|$ and $|\chi^{mag}_{bbb}|$ are the amplitudes of the nonlinear susceptibility of the magnetic terms and δ^{mag}_{abb} and δ^{mag}_{bbb} are the phase shifts between magnetic term and crystallographic term, respectively. The intensity of the SHG signal in the ferromagnetic phase is then given by the following formula:

$$I_{SH} \propto |\chi^{mag}_{bbb}|^2 \cos^2\theta + 2|\chi^{mag}_{bbb}| \cos\theta \sin\theta \left[|\chi^{mag}_{abb}| \cos\varphi \cos(\delta^{mag}_{bbb} - \delta^{mag}_{abb}) + |\chi^{cr}_{cbb}| \sin\varphi \cos\delta^{mag}_{bbb}\right] + \sin^2\theta \left[|\chi^{mag}_{abb}|^2 \cos^2\varphi + 2|\chi^{mag}_{abb}||\chi^{cr}_{cbb}| \cos\varphi \sin\varphi \cos\delta^{mag}_{abb} + |\chi^{cr}_{cbb}|^2 \sin^2\varphi\right] \quad (1)$$

The experimental variations of the signal were fitted using eq 1. The fit of the signal above T_C (Figure 4a) gave access to $|\chi^{cr}_{cbb}|$, and the four other parameters were determined by the

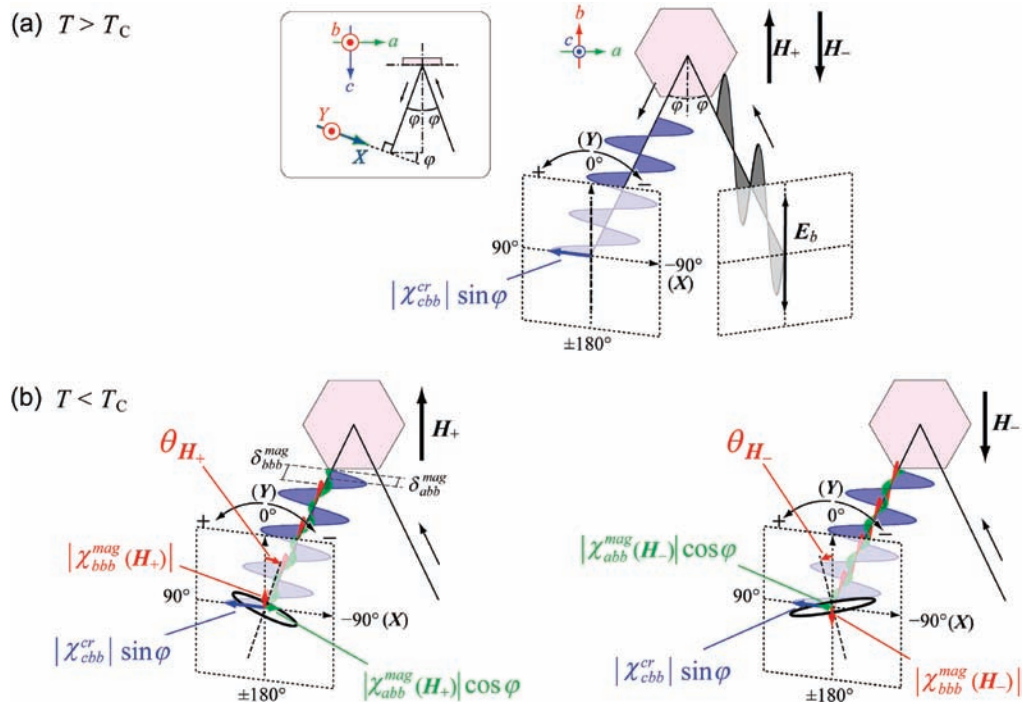

Figure 5. (a) Above T_C, the SHG is related to the single-crystal contribution along the *c* axis (blue). (b) Below T_C, the SHG is influenced by the coexistence of the crystalline contribution (blue) and magnetic contributions along the *a* (green) and *b* (red) axes, leading to elliptically polarized SHG. The inset in (a) shows the single-crystal frame *abc*, with the *c* axis perpendicular to the sample hexagonal surface, and the relevant frame for the SHG wave is *XYZ*, which is rotated by $\varphi = 20°$ around the *b* axis).

Table 1. Parameters Extracted by Using Equation 1 To Fit the Angular Dependence of the SHG Signals Measured at 2 and 20 K (Figure 4) in an External Field of ±0.17 T Applied along the *b* Direction[a]

$\lvert\chi^{cr}_{cbb}\rvert = (20.20 \pm 0.09) \times 10^{-11}$ esu	
$\lvert\chi^{mag}_{abb}\rvert = (3.30 \pm 0.08) \times 10^{-11}$ esu	$\delta^{mag}_{abb} = 80.8 \pm 0.7°$
$\lvert\chi^{mag}_{bbb}\rvert = (1.15 \pm 0.09) \times 10^{-11}$ esu	$\delta^{mag}_{bbb} = 142.5 \pm 5.0°$

[a] The modulus values were converted to esu units using the procedure described in the Supporting Information.

simultaneous fit of the intensities collected at 2 K in a ±0.17 T external magnetic field (Figure 4b), leading to the values collected in Table 1. The fits plotted in Figure 4b indicate that the theoretical expression deduced from the tensorial analysis of the phenomenon is able to reproduce the main features of the evolution of the SHG signal when the material becomes ferromagnetic, (e.g., the variation of the maximum intensity of the signal and its dependence upon the orientation of the magnetization as well as the displacement of the minimum and maximum intensities to angle values different from zero and $\pi/2$, respectively).

The parameters obtained using a simple model considering only the hyperpolarizability effects[24] indicate that the modulus of the magnetization-induced nonlinear susceptibility represents 15% of the crystalline term for $|\chi^{mag}_{abb}|$ and 7.5% for $|\chi^{mag}_{bbb}|$. Moreover, it appears that the phase differences between the magnetic and crystalline contributions are far from the value of $\pi/2$ expected for transparent media.[22] Despite its complexity, it is possible to use eq 1 to determine the influence of the modulus and phase of the χ^{mag}_{abb} and χ^{mag}_{bbb} complex terms on the MSHG. It thus appears that the χ^{mag}_{abb} term of the magnetic nonlinear susceptibility tensor essentially triggers the intensity of the MSHG while the χ^{mag}_{bbb} term plays a key role in the angular shift of the MSHG signal through both its modulus and phase. Let us note that because it allows the phases of χ^{mag}_{abb} and χ^{mag}_{bbb} to depart from $\pi/2$,[22] the absorption of the compound at 532 nm[6] is as an essential feature for the sensitivity of both the MSHG intensity and angular shift upon magnetization reversal. This point is of importance for employing this technique in magnetic domain observation.[25] The present observation will be greatly facilitated relative to the use of linear magneto-optical effects[26] because the angle shift upon magnetization reversal is much larger.[27]

Conclusion

In this paper, we have described the accurate measurement of bulk SHG in an enantiopure chiral magnet as well as MSHG below the Curie temperature of the compound. Thanks to the single-crystalline state of the sample, it has been possible to analyze most confidently the observed properties in a qualitative and a quantitative way by combining tensorial and symmetry

(21) Laughlin, D. E.; Willard, M. A.; Mac Henry, M. E. In *Phase Transformations and Evolution in Materials*; Turchi, P., Gonis, A., Eds.; The Minerals, Metals and Materials Society: Warrendale, PA, 2000; p 121.
(22) Pershan, R. S. *Phys. Rev.* **1963**, *130*, 919.
(23) The label 2_1 indicates a two-fold helical axis combined with time-inversion symmetry.
(24) Fundamental light (1064 nm) and SHG light (532 nm) are partially influenced by chiral, magnetic, and magnetochiral contributions to the optical response in a chiral magnet. Here, these contributions were omitted in the present analysis because their contributions are expected to be small compared with the observed MSHG properties (rotation and ellipticity of SHG light).
(25) Fiebig, M.; Frohlich, D.; Leute, S.; Pisarev, R. V. *Appl. Phys. B: Lasers Opt.* **1998**, *66*, 265.
(26) Ferré, J.; Jamet, J. P.; Pommier, J.; Beauvillain, P.; Chappert, C.; Mégy, R.; Veillet, P. *J. Magn. Magn. Mater.* **1997**, *174*, 77.
(27) (a) Train, C.; Beauvillain, P.; Mathet, V.; Penissard, G.; Veillet, P. *J. Appl. Phys.* **1999**, *86*, 3165. (b) Sato, Y.; Ohkoshi, S.; Arai, K.; Tozawa, M.; Hashimoto, K. *J. Am. Chem. Soc.* **2003**, *125*, 14590.

analysis in both the paramagnetic and ferromagnetic phases. The latter case requires the nontrivial use of the magnetic point group.[7] Using a model limited to hyperpolarizabilities, this analysis has allowed the identification of the parameters that govern the MSHG effect in such materials. It has shown in comparison with linear magneto-optical effects, the magnetic contributions to the nonlinear susceptibility can represent up to 15% of the crystalline one and lead to very large rotation angles. The absorption of the medium for the incoming and/or emitted radiation appears as an important parameter that allows the observation of magnetic domains by MSHG for both out-of-plane and in-plane magnetization.

The measurement and interpretation of bulk MSHG in an enantiopure chiral magnet demonstrates that enantioselective self-assembly of chiral molecular magnets is a demanding but versatile way to design and obtain multifunctional molecular magnets in their crystalline form. Pursuing this strategy will afford new systems that will lead to new MSHG experimental data. The comparison of this enhanced set of data to our model or to more sophisticated ones that include both local and nonlocal effects on the MSHG will lead to a deeper understanding of such optical effects.

Acknowledgment. Dr. K. Takeda is acknowledged for his help in using the SQUID facilities. This work was developed within the framework of the ANR-08-JCJC-0113-01 Project and supported by a grant to C.T. through the Invitation Fellowship Programs for Research in Japan of the Japan Society for the Promotion of Science (JSPS). The present research was also supported in part by a Grant-in-Aid for Young Scientists (S) from JSPS, a grant from the Global COE Program "Chemistry Innovation through Cooperation of Science and Engineering", the Photon Frontier Network Program from MEXT (Japan), and the Murata Science Foundation. It was also supported by the University of Tokyo, UPMC, Univ Paris 06, and CNRS.

Note Added after Print Publication. Because of a production error, the wrong Supporting Information file was included when this article was published ASAP on Nov 2, 2009. The correct Supporting Information file was posted online on Dec 1, 2009.

Supporting Information Available: Measurement of the hysteresis loop at 2 K, measurement of SHG at 293 K, derivation of the nonlinear susceptibility from the powder form measurement, and the complete tensorial analysis of the SHG (above T_C) and MSHG (below T_C). This material is available free of charge via the Internet at http://pubs.acs.org.

JA9061568